

# Study of the Bearing Capacity of Closely Spaced Square Foundations on Granular Soils

William Fuentes · José Duque · Carlos Lascarro · Melany Gil

**Abstract** In the present study, the effect of the interaction between two closely spaced square footings is analyzed through finite element simulations. The numerical analyses were performed through the construction of three-dimensional 3D Boundary Value Problems constructed with the software Abaqus Standard. Several values for the foundation embedment and separation between footings were considered. The behavior of the granular soil was simulated through an extended Drucker–Prager constitutive model. The results were used to calibrate an extended bearing capacity equation through a multiple variable regression analysis, and accounts for the effect of the embedment depth and separation between footings. Finally, the proposed relation was compared with some reported values in the literature, including experimental tests and numerical results, and showed a better agreement with the experimental data than other reported studies.

**Keywords** Closely spaced footings · Bearing capacity · Finite element simulations · Granular soils

## 1 Introduction

The determination of the bearing capacity of the soil is of high importance for the stability of shallow foundations. The literature offers several methods based on the limit equilibrium approach to assess this issue. Since the pioneer work of Terzaghi (1943), a number of enhanced methods, incorporating empirical factors, have been proposed accounting for different effects, such as load inclination, ground inclination, among many others, e.g. Hansen (1961), Meyerhof (1963), Vesic (1973). Nevertheless, very few methods consider the interaction between closely spaced footings. Stuart (1962) studied the effect on the bearing capacity for closely spaced shallow foundations on granular soils and developed an analytical method. This analysis was based on the slip surface proposed by Terzaghi (1943) and assumed limit equilibrium conditions. The authors introduced two new factors in an extended bearing capacity equation, known as the efficiency ratios  $\xi_q$  and  $\xi_\gamma$ , such that:

$$q_u = qN_q\xi_q + \frac{1}{2}\gamma BN_\gamma\xi_\gamma + cN_c \quad (1)$$

where  $q_u$  is the ultimate bearing capacity,  $N_q$ ,  $N_c$  and  $N_\gamma$  are factors depending on the friction angle  $\phi$ ,  $B$  is the shortest dimension of the footing,  $q$  is the initial effective stress at the footings base and  $c$  is the soil cohesion, which for granular soils is set to  $c = 0$ .

Later, West and Stuart (1965) carried out large-scale experimental tests in order to validate the effect

on the bearing capacity  $q_u$  of closely spaced footings, and confirmed that  $q_u$  was indeed susceptible to the separation between them. Robust analytical models, based on a more realistic geometry of the slip surface, were developed to perform accurate predictions. These analyses were carried out considering two or three adjacent footings (Graham et al. 1984; Kumar and Ghosh 2007a, b; Kumar and Saran 2003; Wang and Jao 2002) and found that the maximum bearing capacity for strip footings on sands is achieved when then separation between the footings centers  $S$  takes values between  $S = B$  and  $S = 1.5B$ . Recent studies of other authors investigate the effect of closely spaced footings on different geomaterials: Lavasan and Ghazavi (2008), Abbas and Hussain (2013) considered a reinforced sand with geosynthetics through finite element simulations and analyzed the effect of the separation  $S$ . Noorzad and Manavirad (2014) considered the effect on clays and found a similar, but no equal, pattern as in the case of sands. Other authors analyzed this issue through the use of probabilistic models (Griffiths and Fenton 2006), upper bound limit analyses (Kumar and Ghosh 2007a, b; Kumar and Kouzer 2008; Kouzer and Kumar 2010), lower bound limit analyses (Kumar and Bhattacharya 2013), mathematical models based on linear and nonlinear elastic response of the material (Ghosh et al. 2017) and finite element methods (Lee et al. 2008; Mabrouki et al. 2010; Nainegali et al. 2013; Lavasan and Ghazavi 2014). Experimental studies using scaled tests were performed as well by several authors (Das and Larbi-Cherif 1983; Das et al. 1993; Khan et al. 2006; Kumar and Bhoi 2009; Ghosh and Kumar 2011; Saibaba et al. 2012; Daud 2012; Srinivasan and Ghosh 2013) and found similar results: a maximum bearing capacity is obtained for separations ranging between  $S/B = 1$  and  $S/B = 1.5$ , and it approaches to a value similar to the one of an isolated footing for relations of  $S/B > 4.5$ .

Although these are substantial achievements, they do however lack some additional considerations. First of all, most of them are performed on strip foundations. This means that three-dimensional effects are not considered at all, despite all the current ease provided by numerical tools to assess these effects. Second, very few consider the effect of the embedment depth on the additional factors. This implies that the term of the bearing capacity equation, related to the embedment effect, is not being considered on the

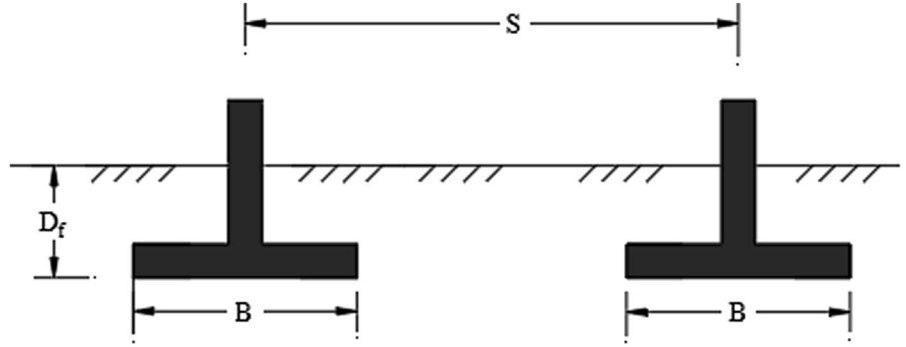
previous analyses. Finally, most of them lack statistical analyses to assure the correct assessment of the new proposed factors for an accurate prediction of the bearing capacity. To the authors' opinion, additional investigation can be performed considering the aforementioned issues.

In the present work, a numerical study of closely spaced square footings was performed to evaluate the influence of the footings separation in the ultimate bearing capacity. For this purpose, finite element simulations considering different embedment depths and separations between the footings were carried out. The selected soil corresponds to a cohesionless sand simulated through an elastoplastic model. With the results, the bearing capacity factors related to the footings separation were calibrated through a linear regression of multiple variables. The article concludes with some final remarks. The tensorial notation of the article is as follows: scalar quantities are denoted with italic fonts (e.g.  $a$ ,  $b$ ), vectors with bold italic fonts (e.g.  $\mathbf{a}$ ,  $\mathbf{b}$ ), second rank tensor with bold fonts (e.g.  $\mathbf{A}$ ,  $\boldsymbol{\sigma}$ ), and fourth rank tensors with special fonts (e.g.  $\mathbf{E}$ ,  $\mathbf{L}$ ). Tensors represented with the indicial notation are denoted with italic symbols with their respective lower indices (e.g.  $A_{ij}$ ,  $\sigma_{ij}$ ). Multiplication with two dummy indices, also known as double contraction, is denoted with colon ":" (e.g.  $\mathbf{A} : \mathbf{B} = A_{ij}B_{ij}$ ). When the symbol is omitted, it is understood a dyadic product (e.g.  $\mathbf{AB} = A_{ij}B_{kl}$ ).

## 2 Brief Description of the Finite Element Model

The finite element model constructed to perform the different numerical analyses is described in the present section. The problem consists of two closely spaced square footings with the following dimensions, see Fig. 1: the width/length of the footings  $B$  is fixed to  $B = 1$  m, the embedment is variable with values of  $D_f = \{0, 1, 2\}$  m, and the separation between footings  $S$  is also variable with values of  $S/B = \{1, 1.5, 2, 2.5, 4\}$  m. Given all the possible combinations, in total, a number of 54 finite element models were constructed and analyzed. The commercial software ABAQUS Standard V6.16 (Dassault Systèmes 2016) was employed for this purpose. The mechanical behavior of the soil was simulated with an elastoplastic model incorporating the Drucker Prager

**Fig. 1** Definition of geometric variables in the problem



yield criterion. Details of this constitutive model is explained in [Appendix](#). Specific details of the Boundary Value Problem are given in the following sections.

## 2.1 Geometry, Mesh and Boundary Conditions

All simulations are three-dimensional 3D and consider a dry granular soil under static analysis. The soil is homogeneous and without cohesion. No inclined loads and/or moments are considered. Its finite element solution is based on the linear momentum equation neglecting the inertial terms (static analysis):

$$\frac{\partial}{\partial x_j} (\sigma_{ij}) + \rho g_i = 0 \quad (2)$$

where  $\sigma_{ij}$  is the (effective) stress tensor,  $\rho$  is the total density and  $g_i$  is the gravity vector. 3D finite elements with linear interpolation were considered. The boundary conditions are shown in Fig. 2 and are as follows: total displacements are restricted on the bottom boundary while horizontal displacements are restricted on the lateral boundaries. Internal mesh

partitions are shown in Fig. 2. The problem domain is 5 m high, 5 m wide and 10 m long as shown in Fig. 3. The problem boundaries were chosen to be far away from the footing to avoid boundary-dependent solutions.

## 2.2 Initial Conditions and Steps of Analysis

Initial conditions assumed oedometric states, such that the initial vertical stresses  $\sigma_{33}$  were computed assuming static equilibrium with a density of  $\rho = 1750 \text{ kg/m}^3$ . Horizontal stresses  $\sigma_{11}, \sigma_{22}$  were computed through the relation  $\sigma_{11} = \sigma_{22} = K_0 \sigma_{33}$ , and using the Jaky's relation for the lateral earth coefficient  $K_0 = 1 - \sin \varphi$ . The analysis begins with a geostatic step to find equilibrium of the initial stresses. Subsequently, the footing was loaded by controlling its settlement. For this purpose, the vertical displacements  $U_3$  of the footing was linearly increased, such that a resulting reaction force was measured. The bearing capacity for this work is understood as the maximum vertical reaction force divided by the footing area.

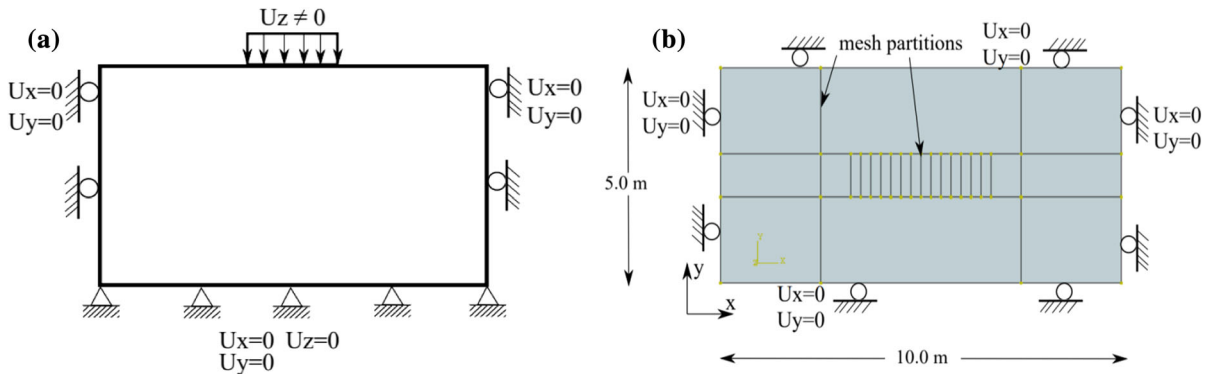


**Fig. 2** a Boundary conditions (side view) and b internal mesh partitions (top view)

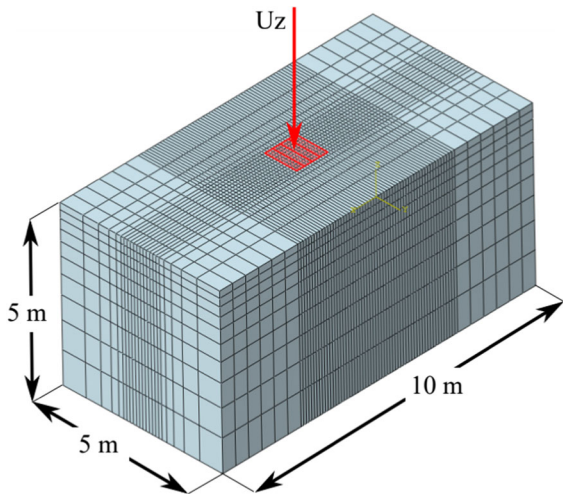


**Fig. 3** Geometry of the boundary value problem (BVP)

The constitutive model for the soil corresponds to an elastoplastic model with linear elasticity, and a yield surface according to an extended Drucker–Prager criterion. This yield surface considers the Lode’s angle dependence according to the equations given in “Appendix”. The flow rule is purely deviatoric, i.e., the dilatancy angle is equal to zero  $\psi = 0$ . The required parameters are the Young modulus  $E$ , the Poisson ratio  $\nu$ , the friction angle  $\varphi$  and the cohesion  $c$ . The first pair defines the elastic response of the soil and material stiffness, while the second controls the material failure. Their values were selected to match some reported data on the literature for typical silty sands under loose, medium and dense state, see Bowles (2001), Obrzud and Truty (2010) and Braja and Sobhan (2016). Table 1 presents a summary of the selected parameters for the simulation. The results of the numerical models are explained in the next section.

**Table 1** Material parameters of constitutive model for a typical silty sand in a loose, medium and dense state

Description		Unit	Loose	Medium	Dense
		Granular soil (extended Drucker Prager model)			
Elastic stiffness					
$E$	Young modulus	MPa	9.5	15	25
$\nu$	Poisson ratio	[-]	0.33	0.31	0.28
Plasticity					
$\varphi$	Friction angle	°	30	34	37
$c$	Cohesion	kPa	0	0	0
Additional parameter					
$\rho$	Density	Kg/m <sup>3</sup>	1450	1550	1750

### 3 Results of the Simulations

The results of the finite element simulations with closely spaced square footings are now analyzed. Figure 4 compiles the results of the bearing capacity  $q_u$  for different  $D_f$ ,  $S/B$  and friction angles  $\varphi$ . Similar to other reported results in the literature (Lavasan and Ghazavi 2012, 2014), they indicate that the effect of a second footing is favorable to the bearing capacity. For the present study, a maximum bearing capacity  $q_u$  was found for a ratio  $S/B$  of approximately  $S/B \approx 1.5$ . This result is corroborated by other works as well (Kumar and Saran 2003; Lavasan and Ghazavi 2008). The bearing capacity recovers the value for isolated footing, denoted by  $q_{u0}$ , for ratios  $S/B$  of approximately  $S/B > 4$ . The ratio  $q_u/q_{u0}$  increases for higher  $\varphi$  values for the studied cases. The results are summarized in Table 2. Figure 5 presents the contours of the deviator stress  $q$  for different separations  $S/B$ . Notice how stress contours indicating an increase of  $q$  are joined together for the case of  $S/B = 1.5$ , see Fig. 5c.

### 4 Calibration of Efficiency Ratios Factors for Bearing Capacity

In this section, the calibration of the equation describing the ultimate capacity  $q_u$  of two closely spaced square footings is explained. The calibration is directly performed with the use of the results in Sect. 3. Let describe the bearing capacity of our problem with Eq. (1) for a cohesionless soil ( $c = 0$ ):

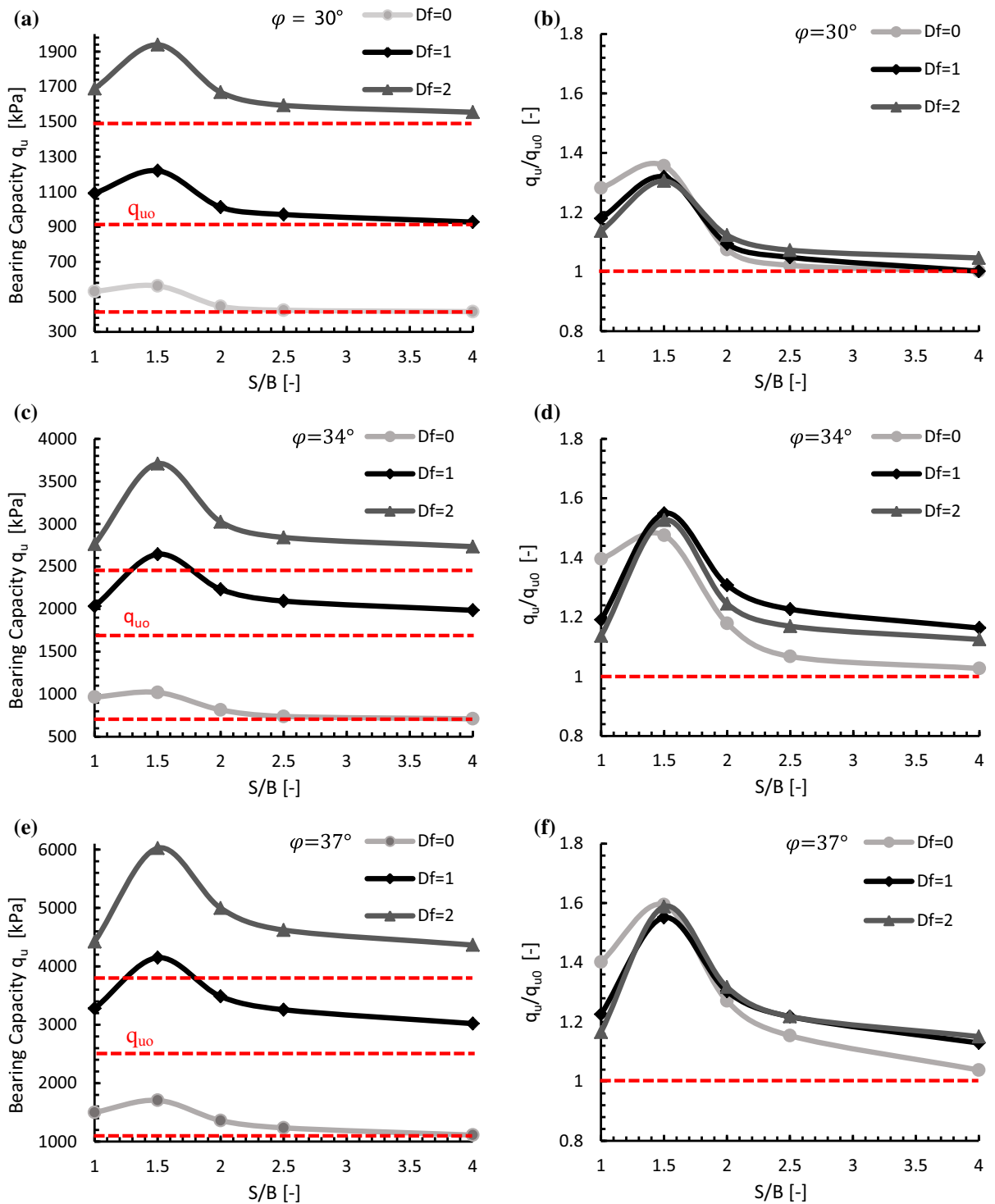


**Fig. 4** Results of the bearing capacity for: **a, b**  $\varphi = 30^\circ$ , **c, d**  $\varphi = 34^\circ$ , **e, f**  $\varphi = 37^\circ$

**Table 2** Results of ultimate bearing capacities  $q_u$  obtained with the finite element simulations

$\varphi(^{\circ})$	$D_f(\text{m})$	$q_{u0}(\text{kPa})$	$q_u(\text{kPa})$ – $S/B$				
			1	1.5	2	2.5	4
30	0	415	532	563	446	424	416
	1	925	1091	1220	1012	970	927
	2	1485	1689	1939	1668	1593	1554
34	0	692	966	1021	816	739	711
	1	1707	2033	2644	2232	2094	1986
	2	2430	2762	3709	3025	2842	2734
37	0	1070	1500	1706	1360	1235	1111
	1	2674	3278	4148	3485	3257	3020
	2	3793	4421	6023	4997	4621	4365

$$q_u = qN_q\xi_q + 0.5\gamma BN_\gamma\xi_\gamma \quad (3)$$

where  $N_q$  and  $N_\gamma$  are factors,  $B$  is the footing dimension,  $q$  is the initial effective stress at the footing's base and  $\xi_q$  and  $\xi_\gamma$  are the efficiency ratios. For calibration purposes, the latter equation may be considered as rigid, in the sense that it demands a first term being proportional to  $q$  and a second term being proportional to  $\gamma$  and  $B$ . Considering this, a generalized form based on the bearing capacity of an isolated footing  $q_{u0}$  and closely spaced footings  $q_u$  was used, such that:

$$q_{u0} = X_q + X_\gamma \quad (\text{for isolated footing}),$$

$$q_u = X_q\xi_q + X_\gamma\xi_\gamma \quad (\text{for closely spaced footings}) \quad (4)$$

where  $X_q$  and  $X_\gamma$  are factors related to the case of an isolated footing, depending on different properties of the boundary value problem, and  $\xi_q$  and  $\xi_\gamma$  are the efficiency ratios depending on the ratio  $S/B$  for closely spaced foundations. In particular, for square footings with dimensions  $B \times B$  and on a soil with fixed material parameters ( $c$ ,  $\varphi$  and  $\gamma$ ), the factors  $X_q$ ,  $X_\gamma$ ,  $\xi_q$  and  $\xi_\gamma$  may be calibrated under the consideration of the following dependencies:

- Factor  $X_\gamma$  is a constant and does not depend on  $D_f$ . It describes the behavior of an isolated footing.
- Factor  $X_q$  is a factor depending on  $D_f$ . It also describes the behavior of an isolated footing.
- Factors  $\xi_q$  and  $\xi_\gamma$  are evaluated for closely spaced square footings, and depend only on the ratio  $S/B$ .

Under these mathematical requirements, the calibration of factors  $X_q$ ,  $X_\gamma$ ,  $\xi_q$  and  $\xi_\gamma$  may be straightforward performed with the following procedure:

- First of all, an isolated footing on the ground surface ( $D_f = 0$ ) is considered, and therefore  $X_q = 0$ . For such conditions, the relation  $X_\gamma = q_{u0}$  holds [see Eq. (4)] and  $X_\gamma$  is solved. This case is illustrated in Fig. 6a.

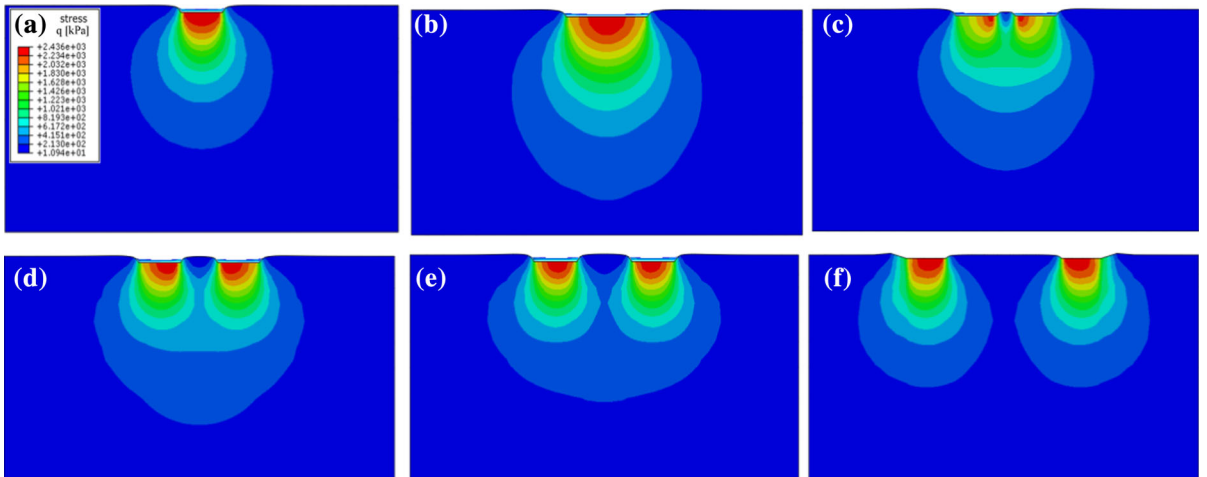


**Fig. 5** Results of the deviator stress  $q$  contours for **a** isolated foundation, **b**  $S/B = 1$ , **c**  $S/B = 1.5$ , **d**  $S/B = 2$ , **e**  $S/B = 5$ , **f**  $S/B = 4$ . All simulations with  $\varphi = 30^{\circ}$

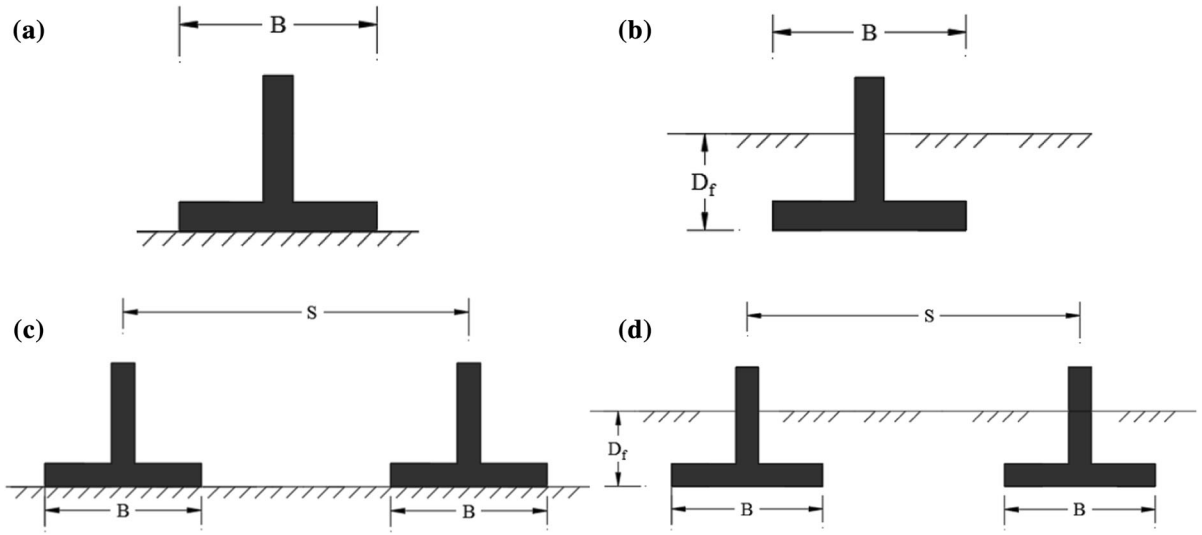


**Fig. 6** Calibration process of the  $\xi_q$  and  $\xi_\gamma$  coefficients: **a** isolated footing with  $D_f = 0$ , **b** isolated footing with  $D_f \neq 0$ , **c** adjacent footings with  $D_f = 0$ , **d** adjacent footings with  $D_f \neq 0$

- (b) Having computed  $X_\gamma = q_{u0}$ , the second factor  $X_q$  is solved for problems of isolated footings with  $D_f > 0$  through the relation  $X_q = q_{u0} - X_\gamma$ , see Fig. 6b. Variation of  $D_f$  must be considered for this calibration.
- (c) With factors  $X_q$  and  $X_\gamma$  already calibrated, the remaining factors  $\xi_q$  and  $\xi_\gamma$  are adjusted through a linear multiple regression analysis considering the results of  $q_u$  for closely spaced square footings with different  $S/B$  and  $D_f$  and constant geomechanical parameters, see Fig. 6c, d.

An example of the multiple regression analysis following the previously described procedure is given in Table 3 and Eq. (5). For that case, factors  $X_q$  and  $X_\gamma$  have been found for an isolated footing considering the variation of  $D_f$ , as described in the aforementioned procedure, see steps (a) and (b). Subsequently, the

**Table 3** Example of data for a multiple regression analysis for  $\varphi = 30^\circ$  and  $S/B = 1$

$D_f$ (m)	$q_u$ (kPa)	$X_q$ (kPa)	$X_\gamma$ (kPa)
0	532	0	415
1	1091	510*	415
2	1689	1070**	415

\*925 – 415, see Table 2; \*\*1485 – 415, see Table 2

calibration of factors  $\xi_q$  and  $\xi_\gamma$  is carried out through a linear multiple regression analysis with the FE results of closely spaced footings. For that purpose, different  $q_u$  are found for each  $D_f$ , considering a fixed value of  $S/B$  and fixed soil's parameters ( $\varphi, \gamma$ ), see e.g. Table 3. These results are transformed into a set of equations, see e.g. Eq. (5), and subsequently, the multiple regression analysis is performed to find factors  $\xi_q$  and  $\xi_\gamma$ . The procedure is repeated for all combinations of  $D_f$ ,  $S/B$  and soil parameters. The accuracy of the regressions was evaluated through the coefficient of determination  $R^2$ . The resulting values of  $R^2$  for all regressions varies within the range  $R^2 = 0.98$  to  $0.99$ , which suggest that Eq. (4) fits accurately to the behavior of closely spaced footings. Figure 7 shows the values of  $\xi_q$  and  $\xi_\gamma$  for each  $S/B$  rendered by the regressions.

$$\begin{aligned}
 532 &= 0\xi_q + 415\xi_\gamma \\
 1091 &= 510\xi_q + 415\xi_\gamma \\
 1689 &= 1070\xi_q + 415\xi_\gamma
 \end{aligned} \tag{5}$$

## 5 Comparison of the Calibrated Equation with Some Reported Results

The obtained results are now compared to some reported data on the literature. Table 4 summarizes

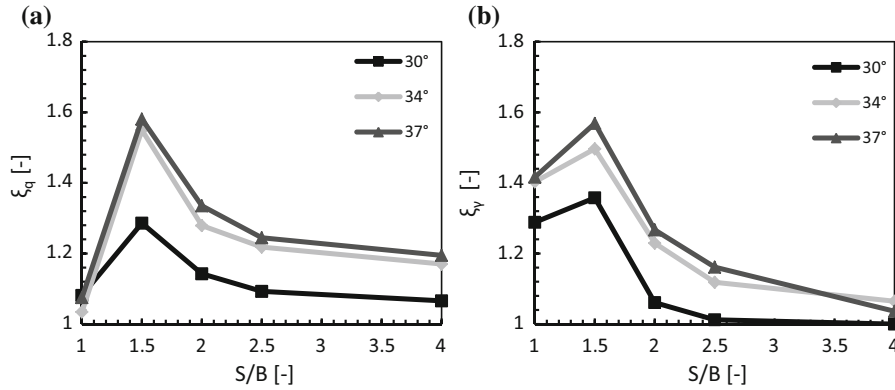


**Fig. 7** Factors **a**  $\xi_q$  **b**  $\xi_\gamma$ , for different friction angles  $\varphi$  after multiple variable regression of the finite element results

**Table 4** Comparison of efficiency factor  $\xi_\gamma$  for closely spaced identical footings, after (Lavasan and Ghazavi 2012)

Footing shape	References	Efficiency factor $\xi_\gamma$				Description
		$S/B = 1$	1.5	2	2.5	
Square	Kumar and Saran (2003)	1.4	1.9	1.4	1.3	Test, $D_f = 60\%$ , $\varphi = 37^\circ$
	Lavasan and Ghazavi (2008)	1.6	2	1.8	1.5	Numerical, $\varphi = 34^\circ$
	Lavasan and Ghazavi (2012)	1.3	1.6	1.2	1.1	Test, $D_f = 40\%$ , $\varphi = 34^\circ$
	Lavasan and Ghazavi (2014)	1.3	1.5	1.1	1.05	Numerical, $\varphi = 37^\circ$
Strip	Stuart (1962)	2	2.6	2	1.7	Theoretical, $\varphi = 35^\circ$
	Das and Larbi-Cherif (1983)	1.8	2	1.7	1.6	Test, $D_f = 54\%$ , $\varphi = 38^\circ$
	Kumar and Ghosh (2007a, b)	2	1.7	1.4	1.2	Theoretical case I, $\varphi = 35^\circ$
		2	2.5	1.9	1.4	Theoretical case II, $\varphi = 35^\circ$
	Kumar and Saran (2003)	2	1.8	1.3	1.2	Test, $D_f = 60\%$ , $\varphi = 37^\circ$
	Mabrouki et al. (2010)	2	1.7	1.2	1	Numerical, $\varphi = 35^\circ$

some information related to different studies of the bearing capacity of closely spaced footings on granular soils for square foundations. Some other studies on strip foundations are also included on the table. The cited works propose equations based on some theoretical considerations, on tests results, or on numerical simulations, see “description” on Table 4. Surprisingly, all analyzed the cases of closely spaced footings on the ground surface, implying that  $D_f = 0$  and that  $\xi_q$  cannot be calibrated. Hence, the present analysis compares only the obtained curve of  $\xi_\gamma$  with the ones reported by the authors.

Figure 8 compares the results of the present study with the ones of Kumar and Saran (2003), Lavasan and Ghazavi (2008, 2012, 2014). Figure 8a compares the resulting factor  $\xi_\gamma$  with the one reported in the

numerical study of Lavasan and Ghazavi (2008) and the experimental study of Lavasan and Ghazavi (2012). The results showed that the present study is able to predict with more accuracy the experiments of Lavasan and Ghazavi (2012) than the study of Lavasan and Ghazavi (2008). Probably, this is due to the fact that the influence of  $D_f$  on factor  $\xi_\gamma$  is herein considered. A similar result is observed in Fig. 8b.

## 6 Final Remarks

In the present study, a bearing capacity equation for closely spaced square footings on granular soils was calibrated. To that end, a statistical analysis on the results of finite element simulations was performed.



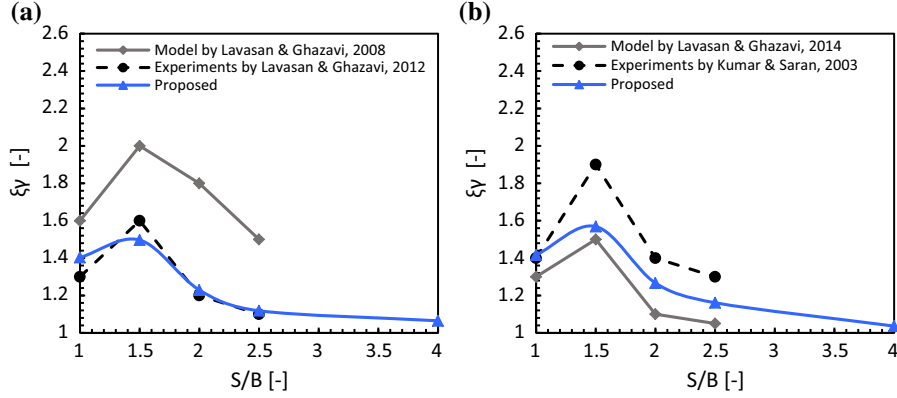


**Fig. 8** Efficiency ratio  $\xi_\gamma$  for different friction angles, **a** for  $\varphi = 34^\circ$ , **b** for  $\varphi = 37^\circ$

The simulations were accomplished with the software Abaqus using an extended Drucker–Prager constitutive model for the soil. The results showed that the bearing capacity  $q_u$  of two closely spaced footings reaches its maximum value  $q_u$  at a separation of approximately  $S/B \approx 1.5$ . In contrast to other works, the statistical analysis performed on the current work considered the calibration of the efficiency factors dependent on the embedment depth and footing’s separation. Comparison of the obtained results with others reported in the literature, suggests that the proposed approach delivers accurate estimations of the bearing capacity factors for closely spaced square footings.

**Acknowledgements** The authors appreciate the financial support given by COLCIENCIAS (Colombia) for the Project with Code 1215748-59323 from the convocation 748-2016, and the one given by the Bolivar Department (Colombia) and administered by Ceiba, through the scholarship “Bolivar wins with science”.

## Appendix

The Drucker–Prager model follows the general equation of an elastoplastic constitutive model:

$$\dot{\boldsymbol{\sigma}} = \mathbf{E} : (\dot{\boldsymbol{\varepsilon}} - \dot{\boldsymbol{\varepsilon}}^p) \quad (6)$$

where  $\dot{\boldsymbol{\sigma}}$  is the stress rate,  $\dot{\boldsymbol{\varepsilon}}$  the strain rate,  $\dot{\boldsymbol{\varepsilon}}^p$  the plastic strain rate and  $\mathbf{E}$  the elastic stiffness (fourth-rank tensor). The plastic strain rate  $\dot{\boldsymbol{\varepsilon}}^p$  is computed considering an extended Drucker–Prager yield surface function  $F$ , defined as:

$$F = t - p \tan \beta - d = 0 \quad (7)$$

where  $t$  is a transformed deviator stress accounting for the Lodes angle  $\theta$  dependence,  $p$  is the mean stress, and  $\beta$  and  $d$  correspond to the modified friction angle and cohesion respectively. Notice that  $\beta$  and  $d$  are functions depending on the classical Mohr–Coulomb parameters  $\varphi$  and  $c$ :

$$\tan \beta = \frac{3\sqrt{3} \tan \varphi}{\sqrt{(9 + 12 \tan^2 \varphi)}} \quad (8)$$

$$d = \frac{3\sqrt{c}}{\sqrt{(9 + 12 \tan^2 \varphi)}} \quad (9)$$

where  $\varphi$  is the friction angle and  $c$  is the soil cohesion. The transformed deviator stress  $t$  is defined as (Dassault Systèmes 2016):

$$t = \frac{1}{2} q \left( 1 + \frac{1}{K} - \left( 1 - \frac{1}{K} \right) \left( \frac{r}{q} \right)^3 \right) \quad (10)$$

where  $r$  is the third stress invariant,  $q$  is the deviator stress, and  $K = M_e/M_c$  corresponds to the ratio between the slope of the yield surface for triaxial extension  $M_e = 6 \sin \varphi / (3 + \sin \varphi)$  and triaxial compression  $M_c = 6 \sin \varphi / (3 - \sin \varphi)$ . The plastic strain rate  $\dot{\boldsymbol{\varepsilon}}^p = \dot{\lambda} \mathbf{m}$  is calculated using the consistency parameter  $\dot{\lambda}$  and a purely deviatoric flow rule  $\mathbf{m} = \partial t / \partial \boldsymbol{\sigma}$ , i.e. the dilatancy angle is equal to zero.  $\nu = 0$  (Dassault Systèmes 2016).

## References

- Abbas J, Hussain I (2013) Bearing capacity of two closely spaced strip footings on geogrid reinforced sand. *Tikrit J Eng Sci* 20(5):8–18
- Bowles J (2001) *Foundation analysis and design*, 5th edn. McGraw-Hill, Peoria
- Braja D, Sobhan K (2016) *Principles of geotechnical engineering*, 9th edn. Cengage Learning, Boston
- Das B, Larbi-Cherif S (1983) Bearing capacity of two closely spaced shallow foundations on sand. *Soil Found* 23(1):1–7
- Das B, Puri V, Neo B (1993) Interference effects between two surface footings on layered soil. *Transp Res Board Record* 1406:34–40
- Dassault Systèmes (2016) *Abaqus theory manual 6.14*. Simulia, Johnston
- Daud K (2012) Interference of shallow multiple strip footings on sand. *Iraqi J Mech Mater Eng* 12(3):492–507
- Ghosh P, Kumar S (2011) Interference effect of two nearby strip surface footings on cohesionless layered soil. *Int J Geotech Eng* 5(1):87–94
- Ghosh P, Rajesh S, Sai J (2017) Linear and nonlinear elastic analysis of closely spaced strip foundations using Pasternak model. *Front Struct Civ Eng* 11(2):228–243
- Graham J, Raymond G, Suppiah A (1984) Bearing capacity of three closely-spaced footings on sand. *Géotechnique* 34(2):173–181
- Griffiths D, Fenton G (2006) Undrained bearing capacity of two-strip footings on spatially random soil. *Int J Geomech* 6(6):421–427
- Hansen B (1961) A general formula for bearing capacity. *Dan Geotech Inst Bull* 11:38–46
- Khan I, Bohara K, Ohri M, Singh A (2006) A study of interference of surface model footings resting on sand. *Inst Eng Malays* 67:15–23
- Kouzer K, Kumar J (2010) Ultimate bearing capacity of a footing considering the interference of an existing footing on sand. *Geotech Geol Eng* 28(4):457–470
- Kumar J, Bhattacharya P (2013) Bearing capacity of two interfering strip footings from lower bound finite elements limit analysis. *Int J Numer Anal Methods Geomech* 37(5):441–452
- Kumar J, Bhoi M (2009) Interference of two closely spaced strip footings on sand using model tests. *J Geotech Geoenviron Eng* 135(4):595–604
- Kumar J, Ghosh P (2007a) Ultimate bearing capacity of two interfering rough strip footings. *Int J Geomech* 1:53–62
- Kumar J, Ghosh P (2007b) Upper bound limit analysis for finding interference effect of two nearby strip footings on sand. *Geotech Geol Eng* 25(5):499–507
- Kumar J, Kouzer K (2008) Bearing capacity of two interfering footings. *Int J Numer Anal Methods Geomech* 32(3):251–264
- Kumar A, Saran S (2003) Closely spaced footings on geogrid-reinforced sand. *J Geotech Geoenviron Eng* 129(7):660–664
- Lavasan A, Ghazavi M (2008) Interference effect of shallow foundations constructed on sand reinforced with geosynthetics. *Geotext Geomembr* 26:404–415
- Lavasan A, Ghazavi M (2012) Behavior of closely spaced square and circular footings. *Soils Found* 52(1):160–167
- Lavasan A, Ghazavi M (2014) Failure mechanism and soil deformation pattern of soil beneath interfering square footings. *Numer Methods Civ Eng* 1(2):48–56
- Lee J, Eun J, Prezzi M, Salgado R (2008) Strain influence diagrams for settlement estimation of both isolated and multiple footings in sand. *J Geotech Geoenviron Eng* 134(4):417–427
- Mabrouki A, Benmeddour D, Frank R, Mellas M (2010) Numerical study of the bearing capacity for two interfering strip footings on sands. *Comput Geotech* 37:431–439
- Meyerhof G (1963) Some recent research of the bearing capacity of foundations. *Can Geotech J* 1:16–26
- Nainegali L, Basudhar P, Ghosh P (2013) Interference of two asymmetric closely spaced strip footings resting on non-homogeneous and linearly elastic soil bed. *Int J Geomech* 13(6):840–851
- Noorzad R, Manavirad E (2014) Bearing capacity of two close strip footings on soft clay reinforced with geotextile. *Arab J Geosci* 7:623–639
- Obrzud R, Truty A (2010) *The hardening soil model: a practical guidebook*. Zace Services Ltd, Lausanne
- Saibaba E, Borzooei S, Narasimha G (2012) Interference between adjacent footings on sand. *Int J Adv Eng Res Stud* 1:95–98
- Srinivasan V, Ghosh P (2013) Experimental investigation on interaction problem of two nearby circular footings on layered cohesionless soil. *Geomech Geoeng* 8(2):97–106
- Stuart J (1962) Interference between foundations with special reference to surface footings in sand. *Géotechnique* 12(1):15–23
- Terzaghi K (1943) *Theoretical soil mechanics*. Wiley, New York, p 510
- Vesic A (1973) Analysis of ultimate loads of shallow foundations. *J Soil Mech Found Div ASCE* 99:45–73
- Wang M, Jao M (2002) Behavior of interacting parallel strip footing. *Electron J Geotech Eng* 7(A):1–10
- West J, Stuart J (1965) Oblique loading resulting from interference between surface footings on sand. In: *Proceedings of the 6th international conference on soil mechanics*, vol 2, pp 214–217